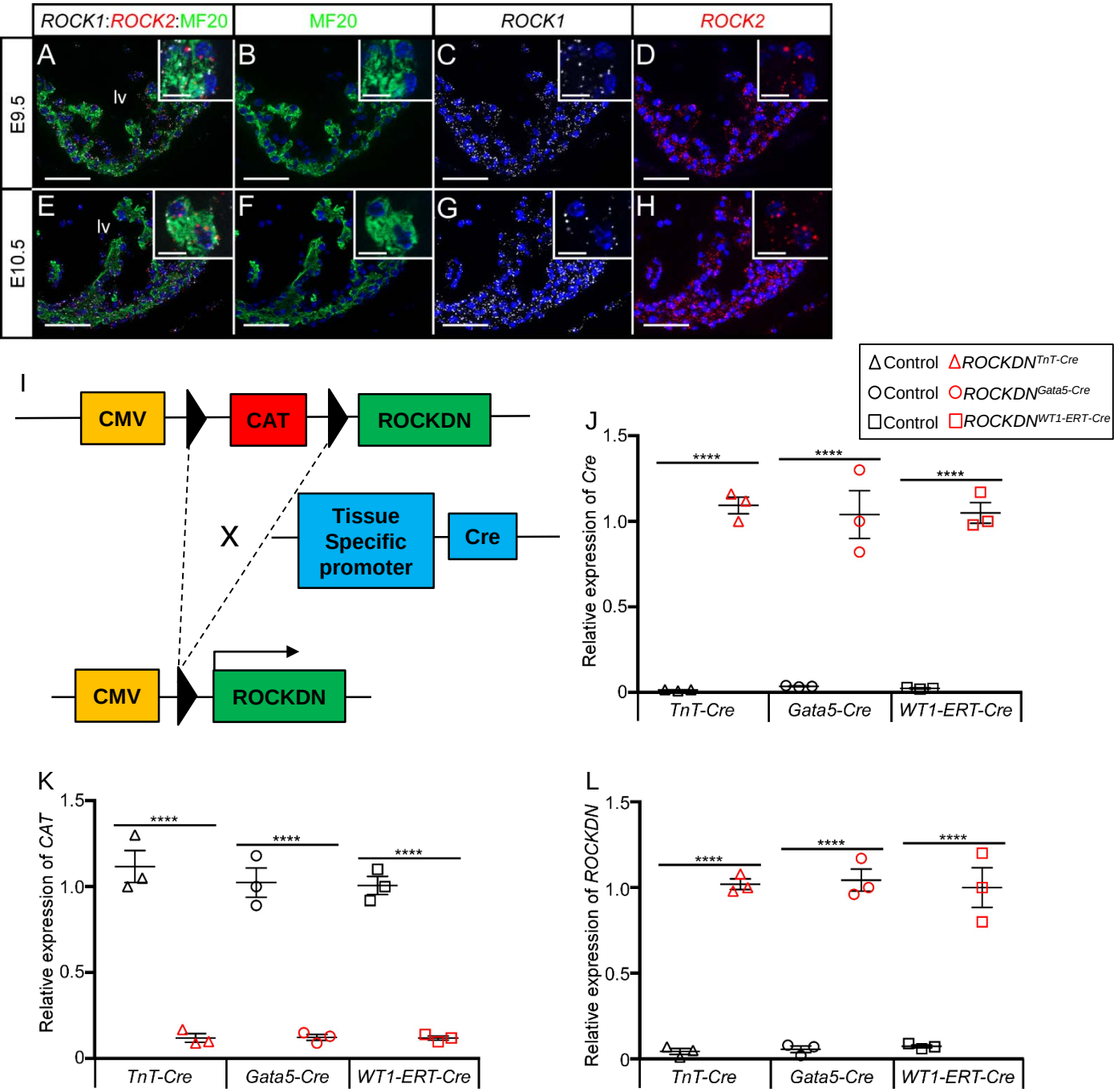


**Supplemental Figure 1: Cardiomyocyte expression of *ROCK1* and *ROCK2*, and activation of *ROCKDN* in the *ROCKDN* transgenic mouse model is dependent upon *Cre* expression.** (**A**-**H**) Using specific *ROCK1* and *ROCK2* probes, RNAscope *in situ* hybridisation showed expression of *ROCK1* (white) and *ROCK2* (red) at E9.5 (**A**-**D**) and E10.5 (**E**-**H**) in the cardiomyocytes throughout the heart. An example from the left ventricular wall is shown here, with a high power magnification of single cells shown in the top right-hand corner of each image. To identify the cardiomyocytes the sections were co-stained by immunofluorescence using MF20 antibody (green) (**B,F**). (**I**) The ROCKDN construct. Expression of *ROCKDN* is inhibited by the presence of the CAT box, which is flanked by LoxP sites. Under the control of cell specific expression of *Cre*, the CAT box is removed, allowing expression of *ROCKDN* and hence downregulating ROCK function in the Cre-activated cells. (**J-L**) cDNA was produced from dissected E15.5 hearts from control (ROCKDN+ve;Cre-ve) and *ROCKDN*$^{Cre}$ mutant (ROCKDN+ve;Cre+ve) littermate embryos and the expression of the *ROCKDN* construct was analysed by qRT-PCR. The expression of *Cre* in each mouse line was confirmed in the *ROCKDN*$^{Cre}$ mutants (**J**). This corresponded with Cre-mediated removal of the CAT box, shown by reduced expression of the *CAT* specific PCR in the *ROCKDN*$^{Cre}$ mutants (**K**). Hence, leading to the specific expression of *ROCKDN*, only in the presence of *Cre* expression for each transgenic *Cre* line (**L**) in the *ROCKDN*$^{Cre}$ mutants . *n*=3 for each genotype. Data are represented as mean ±SEM. ****$P$<0.0001 by one-way ANOVA with Bonferroni correction for multiple comparisons. lv=left ventricle. Scale bar=100μm (**A-H**), 10μm (inset).

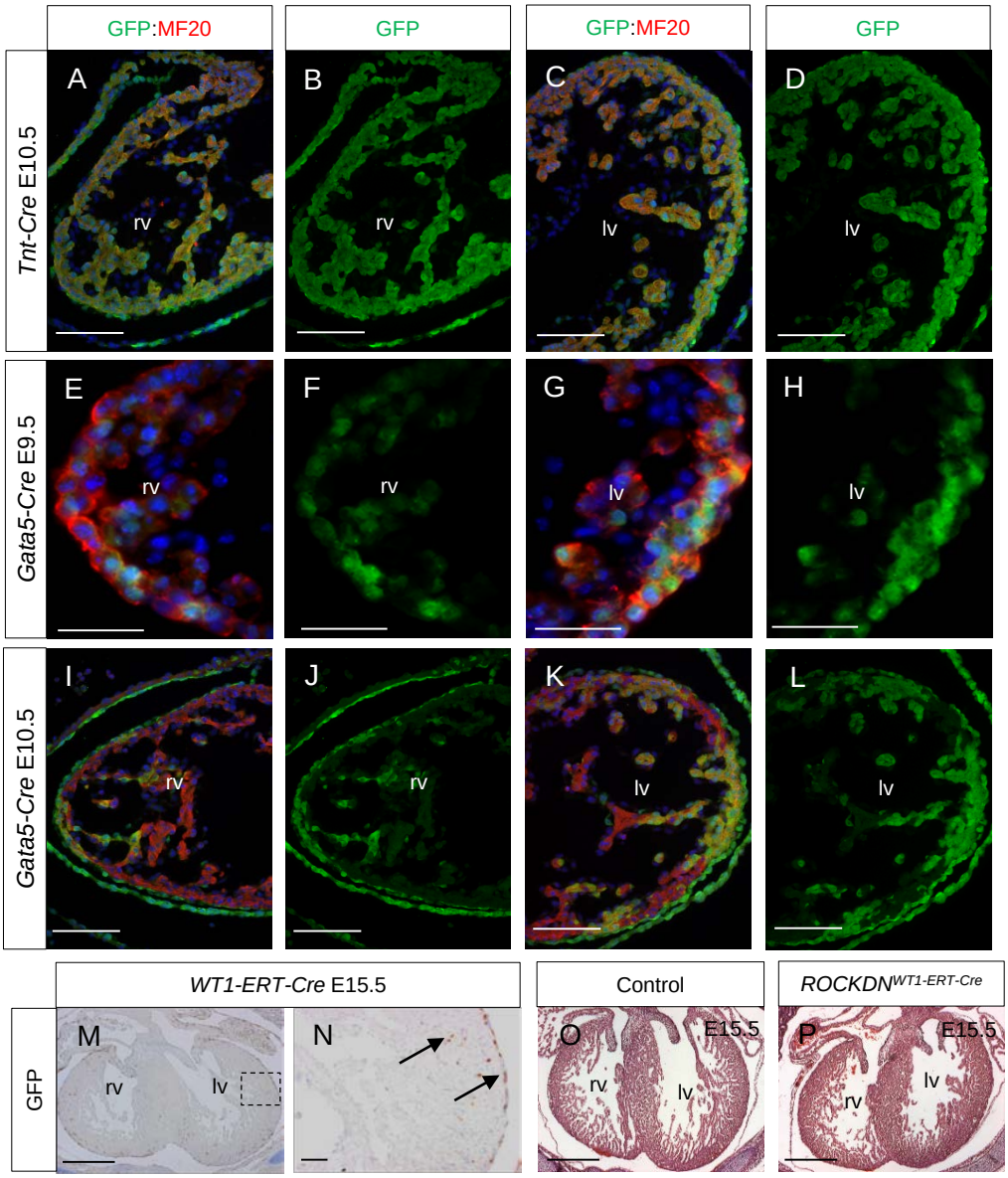





**Supplemental Figure 2: Pattern of Cre expression in the heart in Cre transgenic mouse lines.** (**A**-**L**) Immunofluorescent staining with GFP antibody (green) showing *TnT-Cre* (**A**-**D**) and *Gata5-Cre* (**E**-**L**) expression specifically in the cardiomyocytes (labelled with MF20 antibody (red)) of the developing heart. The average percentage of cardiomyocytes in each ventricle expressing ROCKDN was calculated (see Supplemental Table 1). (**M,N**) DAB immunoreactive staining with GFP antibody confirmed the activation and expression of *WT1-ERT-Cre* in the epicardium and epicardial derived cells (arrows in **N**) at E15.5. (**O,P**) H&E staining showed no difference in heart morphology between control (**O**) and *ROCKDN*$^{WT1\text{-}ERT\text{-}Cre}$ mutant (**P**) hearts. *n*=8 for each genotype. rv=right ventricle, lv=left ventricle. Scale bar=100µm.

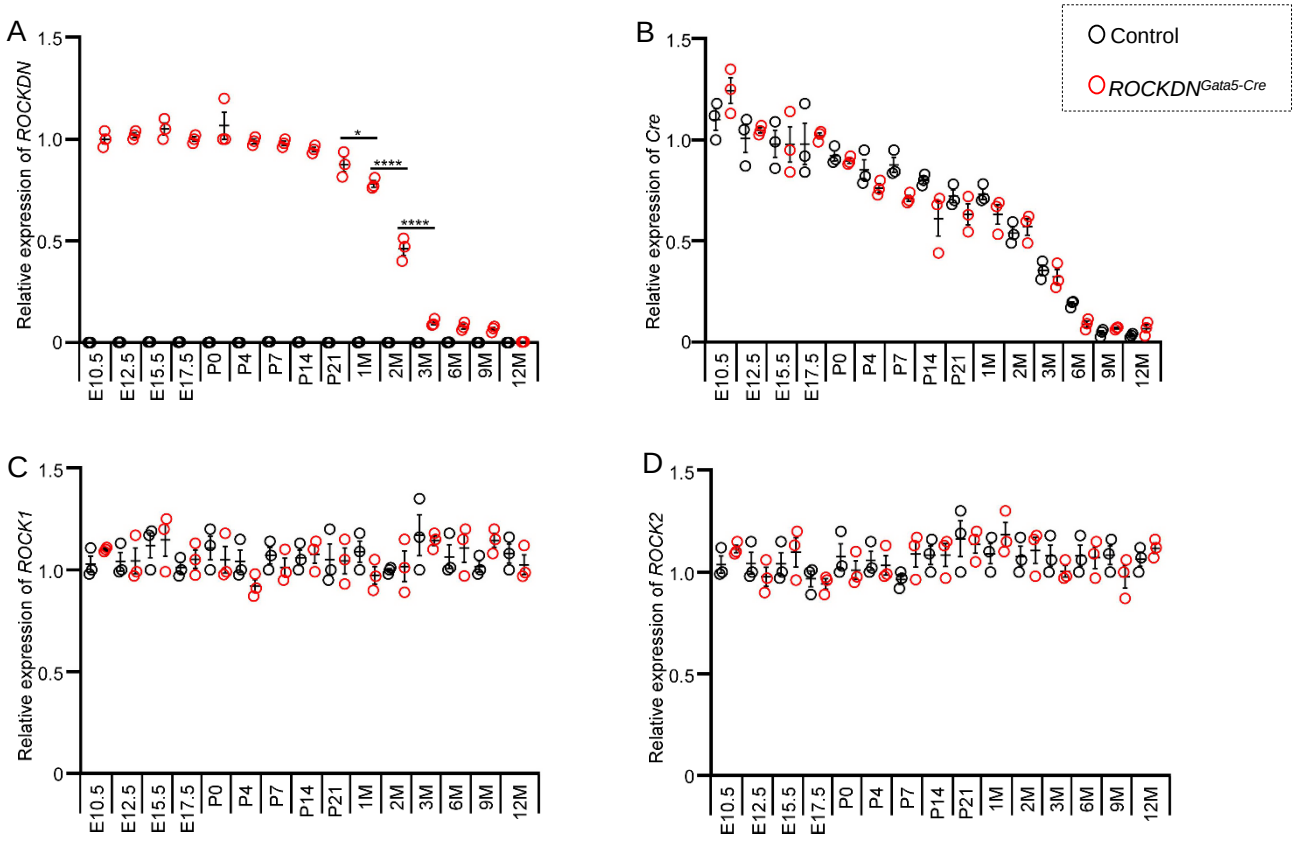


**Supplemental Figure 3: *ROCKDN* is strongly expressed during development and reduced after birth in *ROCKDN*$^{Gata5\text{-}Cre}$ mice but does not alter endogenous *ROCK1* and *ROCK2* expression at any age.** (**A**) qRT-PCR, using RNA extracted from hearts at each time point, from control (ROCKDN-ve;Cre+ve) and *ROCKDN*$^{Gata5\text{-}Cre}$ mutant littermates, showed expression of *ROCKDN* was maintained throughout embryonic developmental with a significant decrease from P21 to 3 months in the *ROCKDN*$^{Gata5\text{-}Cre}$ mutants, after which the level of *ROCKDN* expression remains low. (**B**) There were no significant differences in the level of *Cre* expression between the control and *ROCKDN*$^{Gata5\text{-}Cre}$ mutant samples at each time point, confirming that there was no loss of Cre-activated cells in the *ROCKDN*$^{Gata5\text{-}Cre}$ mutants. (**C,D**) In the same heart samples, qRT-PCR showed no significant difference in endogenous *ROCK1* (**C**) and *ROCK*2 (**D**) expression throughout life between control and *ROCKDN*$^{Gata5\text{-}Cre}$ hearts. *n*=3 for each genotype at all time points. Data are represented as mean ±SEM. **P*<0.05, *****P*<0.0001 by one-way ANOVA with Bonferroni correction for multiple comparisons. M=months.

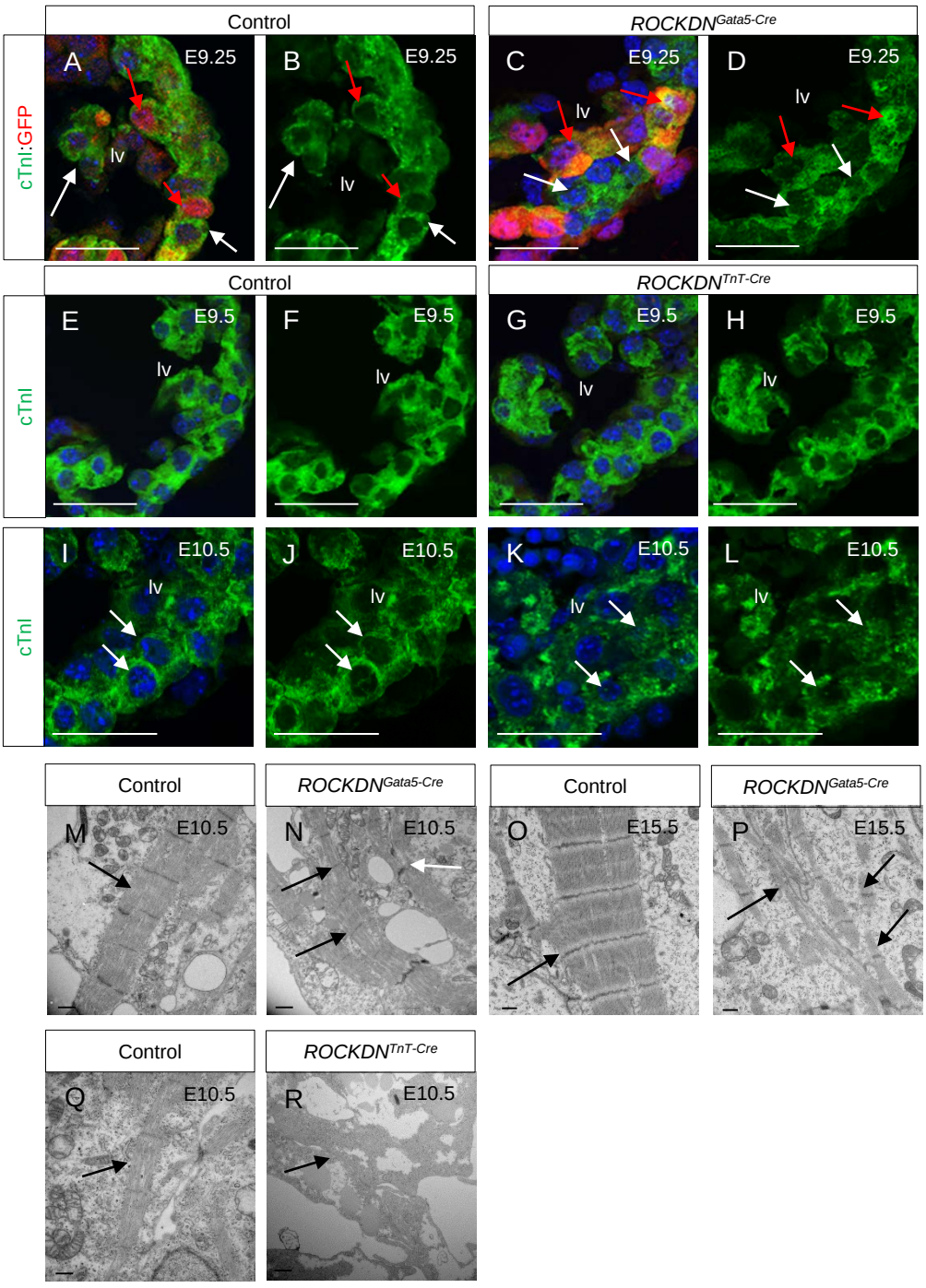


**Supplemental Figure 4: No disruption of sarcomeric proteins in *ROCKDN*$^{Gata5\text{-}Cre}$ mutants at E9.25, and complete disruption of sarcomeres in all cardiomyocytes in *ROCKDN*$^{TnT\text{-}Cre}$ mutants at E10.5.** (**A**-**D**) Immunofluorescent GFP staining (red) at E9.25 confirmed activation of Cre in the GFP+ve cardiomyocytes (red arrows). cTnI staining (green) was comparable between control (**A**-**B**) and *ROCKDN*$^{Gata5\text{-}Cre}$ mutants (**C**-**D**) throughout the ventricular wall in Cre-activated (red arrows) and Cre-negative (white arrows) cardiomyocytes. (**E**-**H**) Immunofluorescent staining showed no difference in cTnI staining at E9.5 in *ROCKDN*$^{TnT\text{-}Cre}$ mutants (**G**-**H**) compared to controls (**E**-**F**). (**I**-**L**) Immunofluorescent staining showed a reduction and disorganisation in cTnI staining at E10.5 in *ROCKDN*$^{TnT\text{-}Cre}$ cardiomyocytes (white arrows in **K**,**L**) compared to controls (**I**,**J**). (**M**-**R**) TEM was used to study the ultrastructure of the sarcomeres. (**M**,**N**) At E10.5, normal sarcomeres (black arrows, **N**) and abnormal sarcomeres (white arrow, **N**) within in the same cardiomyocyte were detected in *ROCKDN*$^{Gata5\text{-}Cre}$ mutants (**N**) and no abnormal sarcomeres were detected in controls (**M**). (**O**,**P**) Sarcomeric defects were still present at E15.5 in *ROCKDN*$^{Gata5\text{-}Cre}$ (arrows in **P**) compared to controls (arrow in **O**). (**Q**,**R**) The sarcomere formation was very abnormal in *ROCKDN*$^{TnT\text{-}Cre}$ mutants at E10.5, with few repeating sarcomeric units present (arrow in **R**) compared to organised sarcomeres in the controls (arrow in **Q**). *n*=3 for each genotype, and *n*=5 for E10.5 *ROCKDN*$^{Gata5\text{-}Cre}$ TEM. lv=left ventricle. Scale bar=50µm. (**A**-**L**) and 500nm (**M**-**R**).

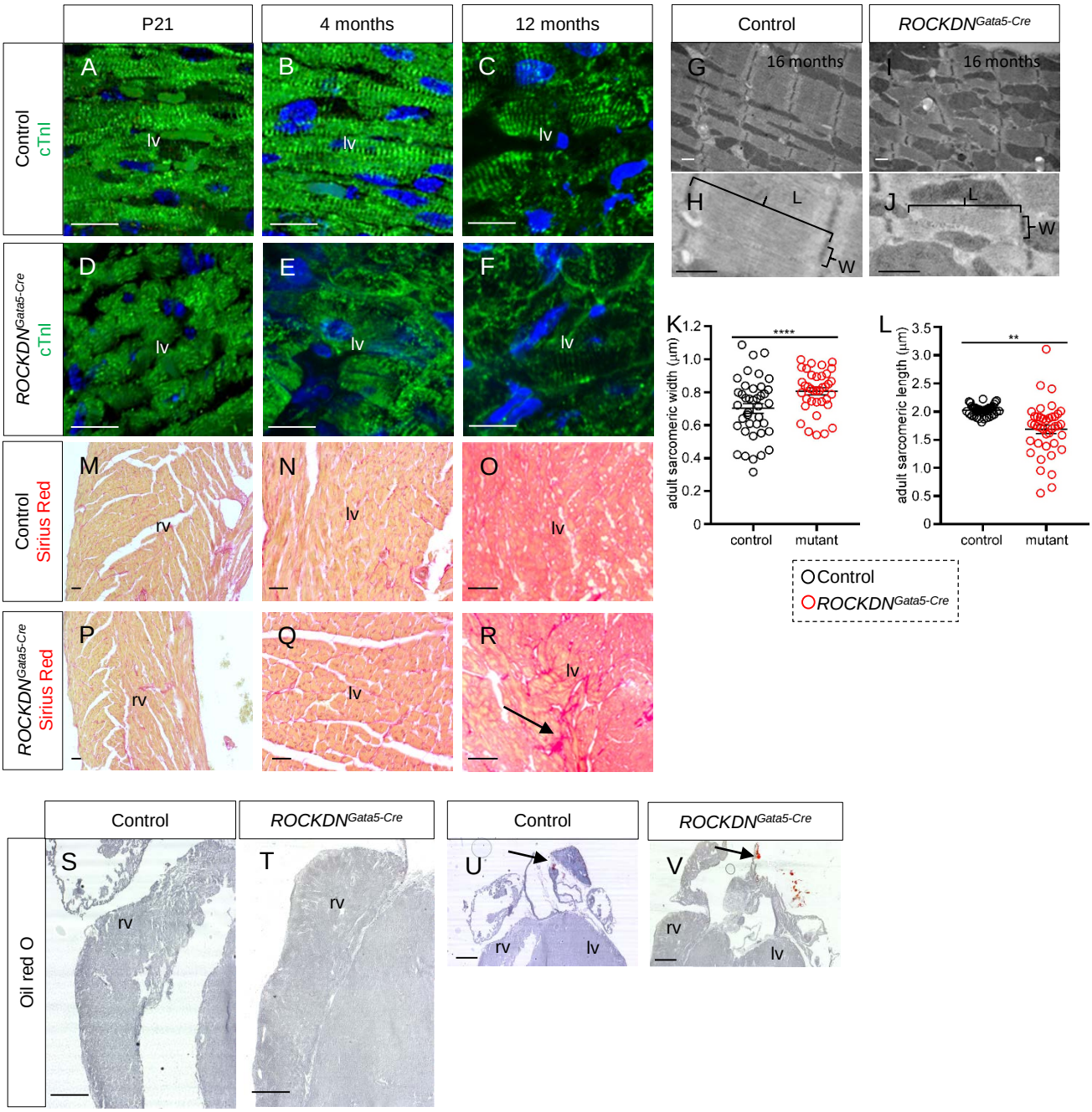





**Supplemental Figure 5: *ROCKDN*$^{Gata5\text{-}Cre}$ mutants display sarcomeric disruption throughout postnatal to adulthood and have fibrosis from 9 months.** (**A-F**) Immunofluorescent cTnI staining showed disorganised sarcomeres with loss of striations in *ROCKDN*$^{Gata5\text{-}Cre}$ cardiomyocytes (**D-F**) at P21 and throughout adulthood compared to control hearts (**A-C**). (**G-J**) TEM analysis showed sarcomere disruption in mutants (**I,J**) compared to controls (**G,H**) at 16 months. Sarcomere length was significantly shorter (**K**) and significantly wider (**L**) in mutants compared to controls. (**M-R**) Sirius red staining for fibrosis showed that there was no fibrosis in *ROCKDN*$^{Gata5\text{-}Cre}$ mutants at P21 and 4 months, whereas at 12 months, similar to 9 months (Figure 9L), patches of fibrosis was seen throughout the ventricular walls. (**S-V**) Oil red O staining showed there was no accumulation of fat deposits in the myocardium of either the control (**S**) or *ROCKDN*$^{Gata5\text{-}Cre}$ mutant (**T**) hearts. Positive oil red O staining was seen elsewhere in the adult heart sections (arrows in **U,V**). *n*=3 for each genotype at each time point. rv=right ventricle, lv=left ventricle, L=length, W=width. ***P*<0.01, ****P<0.0001 by unpaired t test. Scale bar=50μm (**A-F**), 500nm (**G-J**), 100μm (**M-R**) and 500μm (**S-V**).

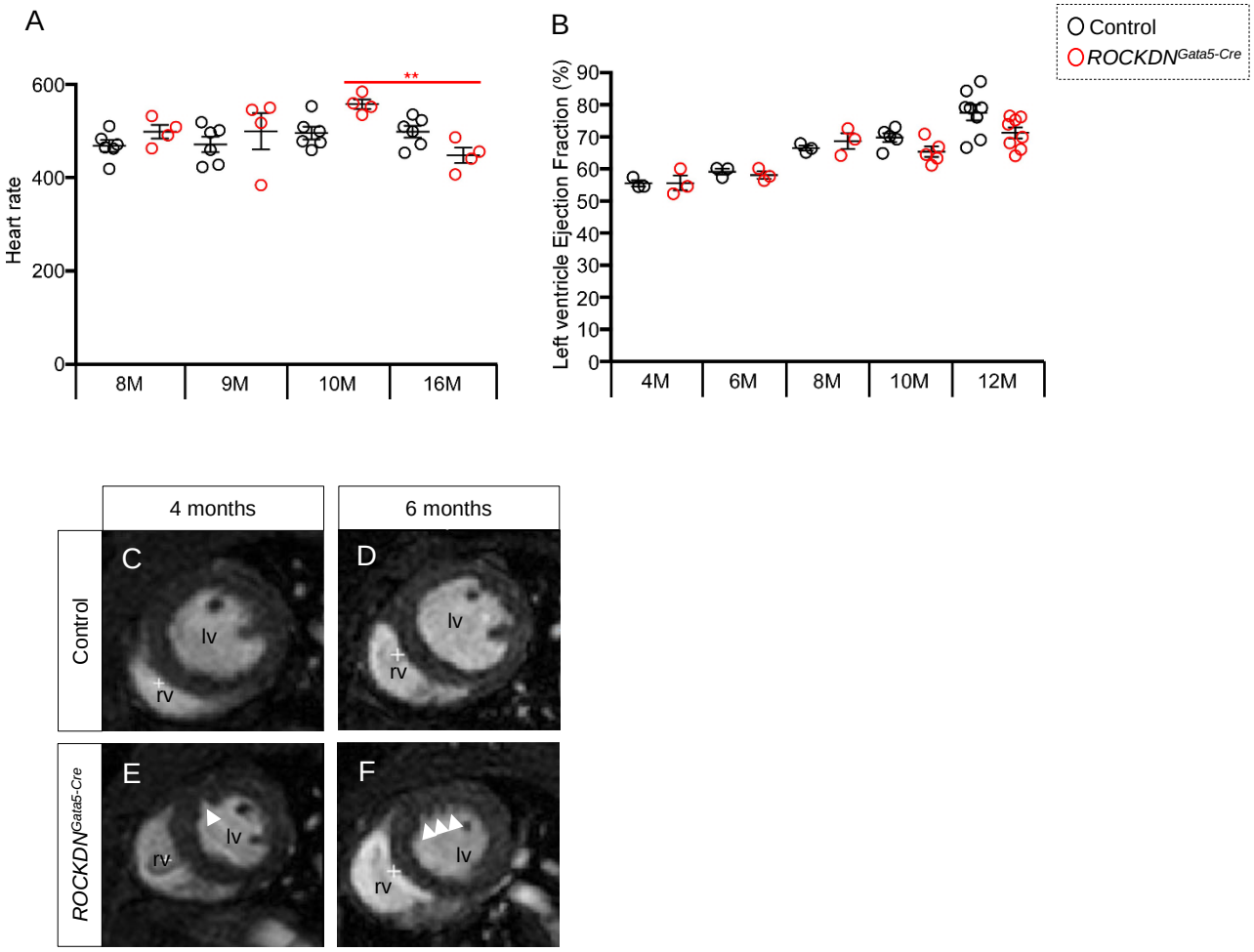


**Supplemental Figure 6: Adult *ROCKDN*$^{Gata5\text{-}Cre}$ mutants display features of hypertrophic cardiomyopathy.** (**A**) The heart rate was measured by ECG and this showed a significant reduction in the heart rate of *ROCKDN*$^{Gata5\text{-}Cre}$ mutants from 10 to 16 months, whereas there was no significant change in the heart rate of control mice over time. *n*=6 for controls, *n*=4 for *ROCKDN*$^{Gata5\text{-}Cre}$ mutants at each time point. (**B**) Cine cardiac MRI analysis showed no significant difference in left ventricular ejection fraction, which was maintained at similar levels in control and *ROCKDN*$^{Gata5\text{-}Cre}$ mice at each age throughout adulthood. *n*=3 for 4 months, *n*=3 for 6 months, *n*=3 for 8 months, *n*=5 for 10 months, *n*=8 for 12 months for each genotype. (**C**-**F**) Myocardial crypts were identified in *ROCKD*$^{Gata5\text{-}Cre}$ MRI images (arrowheads in **E** and **F**) but not in controls (**C,D**). Data are represented as mean ±SEM. ***P*<0.01 by one-way ANOVA with Bonferroni correction for multiple comparisons. rv=right ventricle, lv=left ventricle. M=months.

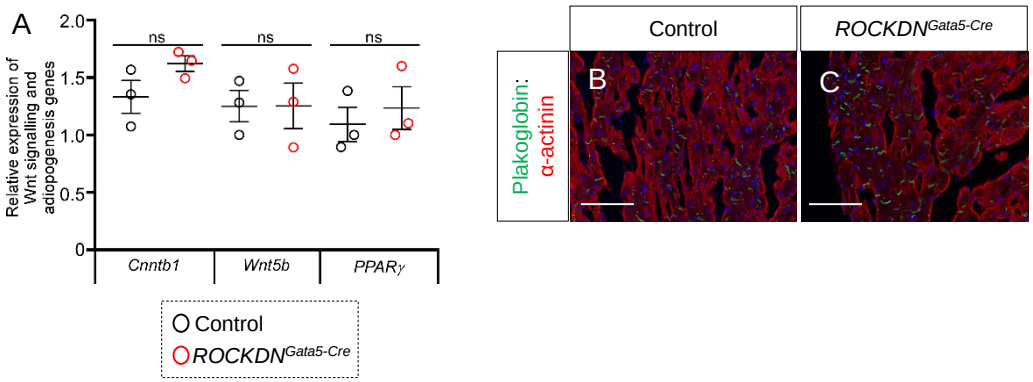


**Supplemental Figure 7: *ROCKDN*$^{Gata5\text{-}Cre}$ mutants do not develop features of arrhythmogenic right ventricular cardiomyopathy.** (**A**) qRT-PCR showed there was no difference in expression of Wnt signalling and adiopogenesis genes between *ROCKDN*$^{Gata5\text{-}Cre}$ mutants and control hearts at 4 months. *n*=3 for each genotype. (**B**-**C**) Immunofluorescent staining showed that at 4 months, plakoglobin staining (green) in the cardiomyocytes (labelled with α-actinin, red staining) was comparable between control (**B**) and *ROCKDN*$^{Gata5\text{-}Cre}$ hearts (**C**). *n*=3 for each genotype. Data are represented as mean ±SEM. ns=non-significant, by one-way ANOVA with Bonferroni correction for multiple comparisons. Scale bar=100µm (**B,C**).

**A**

| *TnT-Cre* | % GFP+ve cardiomyocytes | |
|---|---|---|
| | RV | LV |
| E9.5 | 95 | 91 |
| E10.5 | 97 | 94 |
| E11.5 | 96 | 95 |

**B**

| *Gata5-Cre* | % GFP+ve cardiomyocytes | |
|---|---|---|
| | RV | LV |
| E9.5 | 13 | 19 |
| E10.5 | 18 | 24 |
| E11.5 | 23 | 46 |
| E12.5 | 35 | 54 |
| E15.5 | 55 | 68 |
| E16.5 | 47 | 65 |
| E17.5 | 52 | 67 |

**Supplemental Table 1: Percentage of cardiomyocytes expressing Cre in control and *ROCKDN$^{Cre}$* mutant hearts at different ages.** The Cre-activated cardiomyocytes from *TnT-Cre* (**A**) and *Gata5-Cre* (**B**) hearts, were visualised by GFP and MF20 antibody staining (Supplemental Figure 2). The average percentage of the total number of cardiomyocytes in each ventricle expressing Cre, which equates to the percentage of cardiomyocytes expressing ROCKDN, was estimated by measuring the amount of fluorescent GFP antibody staining in the myocardium compared to MF20 staining (total cardiomyocytes) by ImageJ for different ages throughout development. *n*=3 for all time points.

| A | *ROCKDN*$^{TnT\text{-}Cre}$ | | |
|---|---|---|---|
| **Age** | Total embryos/ pups/ adults | Experimental ratio of *ROCKDN* $^{TnT\text{-}Cre}$ mutants | % lethality of *ROCKDN* $^{TnT\text{-}Cre}$ mutants |
| **E9.5** | 23 | 0.34 | 0 |
| **E10.5** | 198 | 0.27 | 0 |
| **E11.5** | 52 | 0.23 | 8 |
| **E12.5** | 34 | 0.32 | 9 |
| **E13.5** | 57 | 0.18 | 30 |
| **E14.5** | 42 | 0.23 | 40 |
| **E15.5** | 67 | 0.22 | 40 |
| **E16.5** | 37 | 0.14 | 40 |
| **E17.5** | 39 | 0.15 | 34 |
| **P0** | 22 | 0 | 100 |
| **P2** | 6 | 0 | 100 |
| **P4** | 7 | 0 | 100 |

| B | *ROCKDN*$^{Gata5\text{-}Cre}$ | | |
|---|---|---|---|
| **Age** | Total embryos/ pups/ adults | Experimental ratio of *ROCKDN* $^{Gata5\text{-}Cre}$ mutants | % lethality of *ROCKDN* $^{Gata5\text{-}Cre}$ mutants |
| **E9.5** | 43 | 0.37 | 0 |
| **E10.5** | 307 | 0.34 | 0 |
| **E11.5** | 174 | 0.26 | 0 |
| **E12.5** | 99 | 0.28 | 0 |
| **E13.5** | 73 | 0.29 | 0 |
| **E14.5** | 53 | 0.19 | 0 |
| **E15.5** | 481 | 0.22 | 0 |
| **E16.5** | 84 | 0.18 | 0 |
| **E17.5** | 131 | 0.23 | 0 |
| **P0** | 59 | 0.25 | 0 |
| **P2** | 48 | 0.29 | 0 |
| **P4** | 52 | 0.27 | 0 |
| **P7** | 61 | 0.23 | 0 |
| **P21** | 53 | 0.23 | 0 |
| **Adult** | 126 | 0.30 | 0 |

**Supplemental Table 2: Survival of *ROCKDN*$^{TnT\text{-}Cre}$ and *ROCKDN*$^{Gata5\text{-}Cre}$ mutants.** The total number of embryos, postnatal or adult mice collected at each age is shown for the two mouse lines. The proportion of this total, which were either *ROCKDN*$^{TnT\text{-}Cre}$ mutants (**A**) or *ROCKDN*$^{Gata5\text{-}Cre}$ mutants (**B**) was calculated and statistically compared to the expected ratio of 0.25. There was a significant loss of *ROCKDN*$^{TnT\text{-}Cre}$ mutants with no mutants pups collected at birth, ****P<0.0001 by Chi Squared for trend (**A**). There was no significant reduction in the proportion of *ROCKDN*$^{Gata5\text{-}Cre}$ mutants collected at each age (**B**), therefore they all survived to adulthood.

| A | | Average % increase in cardiomyocyte cell size in *ROCKDN*$^{Gata5\text{-}Cre}$ hearts compared to control hearts | |
|---|---|---|---|
| **Age** | ***n*** | **LV (%)** | **RV (%)** |
| **E15.5** | 5 | 7 | 7 |
| **E16.5** | 5 | 16 | 12 |
| **E17.5** | 4 | 16 | 15 |
| **P0** | 3 | 18 | 18 |
| **P4** | 3 | 19 | 19 |
| **P7** | 3 | 22 | 20 |
| **P21** | 4 | 22 | 20 |
| **4M** | 3 | 27 | 22 |
| **9M** | 5 | 43 | 30 |
| **12M** | 5 | 52 | 31 |

| B | Average % increase in cardiomyocyte cell size in *ROCKDN*$^{Gata5\text{-}Cre}$ hearts between ages | | | |
|---|---|---|---|---|
| **Age Range** | **LV (% range)** | **P value** | **RV (% range)** | **P value** |
| **E15.5-E16.5** | 7-16 | 0.160 | 7-12 | 0.394 |
| **E16.5-E17.5** | 16-16 | 0.999 | 12-15 | 0.597 |
| **E17.5-P0** | 16-18 | 0.999 | 15-18 | 0.999 |
| **P0-P4** | 18-19 | 0.999 | 18-19 | 0.999 |
| **P4-P7** | 19-20 | 0.999 | 19-20 | 0.999 |
| **P7-P21** | 22-22 | 0.999 | 20-20 | 0.999 |
| **P21-4M** | 22-27 | 0.502 | 20-22 | 0.999 |
| **4M-9M** | 27-43 | <0.0001**** | 22-30 | 0.962 |
| **9M-12M** | 43-52 | 0.024* | 30-31 | 0.999 |

**Supplemental Table 3: All cardiomyocytes in the *ROCKDN*$^{Gata5\text{-}Cre}$ mutants were significantly hypertrophic from E16.5, with a further specific asymmetrical increase in the LV from 9 months.** (**A**) The area of individual cardiomyocytes was calculated using WGA staining and ImageJ analysis (see Figure 3K,L and Figure 8A,B). The percentage increase in the average cardiomyocyte cell size in the *ROCKDN*$^{Gata5\text{-}Cre}$ mutants compared to the control hearts was calculated. In both the left and right ventricles, the increase in cell size was significantly different in the mutants compared to controls from E16.5. (**B**) The increase in cardiomyocyte cell size in the *ROCKDN*$^{Gata5\text{-}Cre}$ mutants was compared between 2 consecutive ages. In the left ventricle there was a significant increase in cell size from 4 to 9 months and from 9 to 12 months, which was not observed in the right ventricle. **P*<0.05, *****P*<0.0001 by one-way ANOVA with Bonferroni correction for multiple comparisons.

## Supplemental Methods

**Supplemental Table 1: Genotyping primers for mouse lines.**

| Genotyping Primers | Primer Sequence (5'-3') |
|---|---|
| RhoA-forward | ACT CAT CTC AGA AGA GGA TCT G |
| RhoK- reverse | TTC ATT CAG TTC TTT CTG ATA TTT G |
| Cre-forward | GCA TAA CCA GTG AAA CAG CAT TGC TG |
| Cre- reverse | GGA CAT GTT CAG GGA TCG CCA GGC G |

**Supplemental Table 2A: Primary Antibodies.**

| Primary Antibodies | Company: catalogue number |
|---|---|
| BrdU | Abcam: ab6326 |
| GFP | Torrey Pines: TP401 |
| GFP | Abcam: ab13970 |
| cTnI | Hytest: 4T21/2 |
| α-SMA | Sigma Aldrich: A2547 |
| MF20-c | The Developmental Studies Hybridoma Bank |
| Plakoglobin | Abcam: ab184919 |
| α-actinin EA-53 | Sigma Aldrich: A7811 |
| DNase1, Alexa Flour ™ 488 conjugate | Life Technologies: D12371 |
| Phalloidin Alexa Fluor™ 594 conjugate | Life Technologies: A12381 |

**Supplemental Table 2B: Secondary Antibodies.**

| Secondary Antibodies | |
|---|---|
| Alexa Fluor™ Anti-chicken IgG(H+L) 488 | Life Technologies: A11039 |
| Alexa Fluor™ Anti-Rabbit IgG(H+L) 594 | Life Technologies: A21207 |
| Alexa Fluor™ Anti-Mouse IgG(H+L) 594 | Life Technologies: A21203 |
| Alexa Fluor™ Anti-Goat IgG (H+L) 488 | Life Technologies: A32814 |
| Alexa Fluor™ Anti-Mouse IgG(H+L) 488 | Life Technologies: A21202 |
| Anti-mouse biotinylated | Dako: E0354 |

**Supplemental Table 3: qRT-PCR primer sequences.**

| qRT-PCR primers | Primer sequence (5'-3') |
|---|---|
| ANF-forward | GAGAGAAAGAAACCAGAGTG |
| ANF-reverse | GTCTAGCAGGTTCTTGAAATC |
| CAT-forward | CAGTCAGTTGCTCAATGTACC |
| CAT- reverse | ACTGGTGAAACTCACCCA |
| Cnntb1- forward | CCTAGCTGGTGGACTGCAGAA |
| Cnntb1-reverse | CACCACTGGCCAGAATGATGA |
| Cre-forward | GCATAACCAGTGAAACAGCATTGCTG |

| | |
|---|---|
| Cre-reverse | GGACATGTTCAGGGATCGCCAGGCG |
| Gapdh-forward | TGTGCAGTGCCAGCCTCGTC |
| Gapdh-reverse | TGACCAGGCGCCCAATACGG |
| Myh7- forward | AGAACAAACTGAGGCGTGGG |
| Myh7- reverse | CCAGTGCCTTTCCGAACAAT |
| Phospholamban-forward | CGATCACCGAAGCCAAGGTCTC |
| Phospholamban-reverse | GTGGCGGCAGCTCTTCACAGA |
| Pparγ-forward | TGTCGGTTTCAGAAGTGCCTTG |
| Pparγ-reverse | TTCAGCTGGTCGATATCACTGGAG |
| ROCK1- forward | AACGCTGTCAACAAGATCCAC |
| ROCK1- reverse | CACATGATTCCAACACAGCAG |
| ROCK2-forward | TGGTTACTATGGGCGAGAATG |
| ROCK2-reverse | TCTGCGTAAAATGGAGTGTCC |
| ROCKDN-forward | TGGAACAAAAACTCATCTCAGAA |
| ROCKDN-reverse | TGCAAGATTGGCAACATCAC |
| Skeletal actin- forward | TCCAAGTCCTGCAAGTGAACA |
| Skeletal actin- reverse | CTTCGTCGCACATGGTGTC |
| Wnt5b-forward | CTCTCATGAACCTACAGAACAACGA |
| Wnt5b-reverse | TGGAGCCAGCAGGTCTTGA |

**Supplemental Table 4. Primary antibodies for Western Blot and Co-IP.**

| **Primary Antibodies for Western Blot** | **Company: catalogue number** |
|---|---|
| ROCK1 | Abcam: ab45171 |
| ROCK2 | Abcam: ab125025 |
| cTnI | Hytest: 4T21/2 |
| TnT | Abcam: ab125266 |
| Mlc2 | Abcam: ab92721 |

**Supplemental Table 4B: Secondary antibodies for Western blot and Co-IP.**

| **Secondary Antibodies For Western Blot** | |
|---|---|
| Horse radish peroxidase Goat | Dako: P0449 |
| Horse radish peroxidase Rabbit | Dako: P0448 |

**Supplemental Methods**:

*Mice*. All the mice used in this study were on a C57Bl6 background and had been backcrossed more than 5 times and for breeding they were a minimum of 8 weeks old. Only females were kept for all of the analysis performed on adult animals. Cardiac specific *Cre* mouse lines were used to specifically target ROCK downregulation during cardiac development. The *TnT-Cre* promoter is expressed from E7.5 and is restricted to the cardiomyocytes of the myocardium (1). *Gata5-Cre* mice (2) were used to target ROCK activity in the myocardium and the epicardium; *Cre* activity is activated from E9.25. To target ROCK activity in the epicardium the

tamoxifen inducible *WT1-ERT-Cre* mice (3) were used. For the latter, *Cre* expression was activated via the administration of 2 consecutive daily Tamoxifen (100mg/ml) injections. Tamoxifen was administrated intraperitoneally to pregnant dams at E9.5 and E10.5. Mice containing a dominant negative ROCK mutant (CAT-Rho-KDN/3-1, BRC_No 01294) were originally obtained from the RIKEN BioResource Center (Tsukuba, Japan) (4). *ROCKDN* mice were inter-crossed with *R26ReYFP* reporter mouse line (5) producing *ROCKDN$^{eYFP}$* mice. *eYFP* mice contain a transcriptional stop sequence flanked by *LoxP* sites, enabling the identification of Cre-activated cells, and thus ROCKDN expression, by the presence of YFP, which is detected using a GFP antibody. These mice were then crossed with the cardiac specific *Cre* mouse lines, either: *TnT-Cre*, *Gata5-Cre* or *WT1-ERT-Cre* to obtain *ROCKDN* mutant mice (ROCKDN$^{+/-}$;TnT-Cre$^{+/-}$: (known as *ROCKDN$^{TnT-Cre}$*), ROCKDN$^{+/-}$;Gata5-Cre$^{+/-}$: (known as *ROCKDN$^{Gata5-Cre}$*) and ROCKDN$^{+/-}$;WT1-ERT-Cre$^{+/-}$: (known as *ROCKDN$^{WT1-ERT-Cre}$*). Littermates lacking the *ROCKDN* mutant allele and/or Cre negative littermates (ROCKDN$^{-/-}$Cre$^{+/-}$, ROCKDN$^{-/-}$;Cre$^{-/-}$, ROCKDN$^{+/-}$;Cre$^{-/-}$, ROCKDN$^{+/-}$;Cre$^{+/-}$) were used as controls as they were all confirmed as phenotypically normal. Genotyping was confirmed by PCR amplification of ear-clip, limb or yolk sac DNA.

*Collection of Mouse embryos*. Male *Cre* mice were mated with female *ROCKDN$^{eYFP}$* mice. Females were examined for the presence of a copulation plug the following morning. For approximate embryo staging, detection of plug was deemed E0.5. Pregnant dams were sacrificed by cervical dislocation and embryos at different ages were dissected at noon on day of collection.

*Histology*. For histology, all embryos (E9.5-E17.5) and postnatal hearts (P0-P21) were fixed in 4% paraformaldehyde and then processed through a series of ethanols and embedded in paraffin. Adult hearts were dissected in PBS and then processed through 7.5% sucrose and 15% sucrose before being embedded in OCT and frozen at -80°C. Embryos were sectioned transversely and hearts coronally prior to staining.

*IF and IHC expression quantification*. αSMA and Cre expression were calculated as a percentage of the total number of cardiomyocytes. Analysis was performed using transverse four chambered view sections. Image J software was used for analysis, a total of 3 sections per heart were analysed and then the average calculated. The investigator was blinded to genotype of samples for the analysis of the results.

*Cardiomyocyte size*. Cardiomyocyte area was calculated in E15.5, E16.5, E17.5, P0, P4, P7 and P21 and adult (4M, 9M and 12M) hearts. Paraffin sections were deparaffinised and adult heart cryosections were fixed in 4% paraformaldehyde for 10 minutes then washed in PBS. Cell membranes were stained with fluorescently conjugated WGA at room temperature for 1 hour. Sections were imaged on an Axioimager2 (Zeiss). Individual cardiomyocyte area was measured using Image J software. A total of 3 sections, and on average 900 cells were analysed per heart. Only cardiomyocytes in a transverse orientation, adjacent to transversely sectioned capillaries, were measured. The investigator was blinded to the genotype of the samples for the analysis of the results.

*Ventricular wall and Trabecular complexity measurements.* All measurements were taken using transverse sections in a four chambered view and the investigator was blinded to the genotype of the samples for the analysis of the results. For embryonic hearts, images were captured at x2.5 magnification to capture the entire heart and chest cavity. For postnatal and

adult hearts, whole heart tiled images captured at x2.5 magnification were generated. For wall thickness measurements the ventricle wall was imaged at x20 magnification. Measurements were performed using Image J software. In total, 3 sections were analysed per heart. For each section, 3 measurements were taken for the LV and RV myocardial wall, averaged and then normalised to the thoracic cavity width (embryonic hearts) or heart height (postnatal and adult hearts). Trabecular complexity was calculated by dividing the length of each trabeculae by its thickness. 3 sections were analysed per heart, multiple measurements were taken throughout the myocardium of both the LV and RV and the average calculated.

*TEM measurements*. Images were generated from tissues blocks and sarcomere length, width, Z band width, and the angle at which sarcomeres approached the intercalated disk were measured and the number of repeating sarcomeric units were also counted. The myofibril and G actin density were calculated as a percentage of total cardiomyocyte area. All analysis was performed using Image J software. A total of 40 individual sarcomeres were measured per heart and the average was calculated.

*RNAscope*. *ROCK1* and *ROCK2* mRNA expression was examined by RNA *in situ* hybridisation using RNAscope ® Multiplex Fluorescent v2 Assay (Advanced Cell Diagnostics, Newark, CA, USA) following manufacturer's instructions. E9.5 and E10.5 embryos were fixed overnight at 4°C in 4% paraformaldehyde and paraffin embedded. Tissues were sectioned at 8µm and deparaffinised. Antigen retrieval was performed using RNAscope® Target Retrieval Reagent (95°C for 5 minutes for E9.5 embryos and 15 minutes for E10.5 embryos) and ACD Protease Plus reagent (40°C for 5 minutes for E9.5 embryos and 15 minutes for E10.5 embryos). The targeting probes Mm-Rock1-C2 (Cat No. 526271-C2) and Mm-Rock2 (Cat No. 507971) were incubated on sections for 2 hours at 40°C, and following this, the RNAscope signal was amplified using ACD AMP1-3 and then visualised using TSA-based fluorophores (TSA Plus Cyanine 3, PN NEL744001KT, TSA Plus Cyanine 5, NEL745001KT, Perkin Elmer). Following the RNAscope assay, sections were stained by immunofluorescence. To identify cardiomyocytes, sections were incubated at 4°C overnight with MF20 primary antibody (Dev Hyb Bank) and then incubated 2 hours at room temperature with secondary antibody (Alexa Fluor™ Anti-Mouse IgG (H+L) 488, Life tech) and mounted with ProLong™ Gold Antifade Mountant with DAPI (Invitrogen™).

*HREM*. To minimise retention of blood, harvested embryos were agitated in warmed (37°C) PBS containing heparin for 15 minutes and umbilical vessels continually clipped to enable blood to be pumped out. Potassium chloride (final 50mM) was added to arrest hearts in diastole. Hearts (including lungs and thymus) were dissected, washed in PBS, one lung lobe removed and the hearts were fixed for 30 minutes in 4% paraformaldehyde at 4°C. Remaining blood was removed through repeated washes in changes of distilled water over 1 hour at room temperature with constant agitation. Hearts were further fixed overnight in 4% paraformaldehyde at 4°C. Hearts were then dissected from the lung and thymus prior to dehydration in ethanol series.

*Cardiomyocyte isolation*. Hearts were dissected from E15.5 or E17.5 embryos and placed into ice cold cardiomyocyte balanced salt buffer (CBSB) (NaCl, HEPES, $NaH_2PO_4$, KCl, $MgSO_4$, pH7.4) and were cut into fragments. These fragments were placed in a sterile 15ml tube and dissociated in enzyme solution (100ml CBSB solution with 80U/ml Collagenase Type 2 and 0.25mg/ml trypsin) at 37°C for 5 minutes. This was centrifuged and the supernatant was

collected and cells re-suspended in foetal calf serum (FCS). Enzyme solution containing trypsin (0.25mg/ml) was then added to the remaining tissue fragments and incubated at 37°C for 30 minutes with gentle agitation every 10 minutes. Following incubation, the fragments were allowed to settle and supernatant collected, and fresh enzyme solution added to remaining fragments. This process was repeated until all of the heart fragments were fully dissociated. Cells were then pre-plated on collagen coated flasks at 37°C for 2 hours in cardiomyocyte growth media (DMEM, Medium 199, FCS, horse serum, pen/strep) to remove the fibroblasts. Media containing the cardiomyocytes was collected from the pre-plating flask and then plated on collagen-coated flasks. After 48 hours, the media was discarded and cells gently washed 2-3 times with PBS to remove debris and dead cells. To assess the effect of ROCK downregulation on cardiomyocytes, isolated cells were then treated with ROCK inhibitor Y27632 (final concentration 10µM) and cultured for 24 hours. 3-siobutyl-1-methylxanthine (IBMX) (Sigma, 15879-100MG) treatment was performed on cardiomyocytes isolated from *ROCKDN*$^{Gata5\text{-Cre}}$ control and mutant hearts. Isolated cardiomyocytes were serum starved for 24 hours prior to IBMX treatment (final concentration 0.6µM) and then cultured for 24 hours. Cells where then washed in PBS and fixed in 4% PFA. IF was performed; cardiomyocytes were washed and blocked and stained with appropriate antibody (Supplemental Table 2) and counterstained with DAPI and then imaged using Nikon A1R confocal. Experiments were repeated using 4 biological replicates. Image J was used to measure cardiomyocyte area and fluorescent intensity.

*MRI*. Mice were anaesthetised with 5% isofluorane, then shaved and laid prone on a cradle (Dazai Research Instruments, MICe, Toronto, Canada) allowing monitoring of heart rate, respiratory rate and body temperature. Mice were placed in the magnet and anaesthesia was maintained using 1-1.8% isofluorane via a nose cone. Warm air was blown into the magnet to maintain body temperature. A 7 Tesla horizontal bore Varian microimaging system equipped with a 12 cm microimaging gradient insert (maximum gradient 40 Gauss/cm) (Varian Inc., Palo Alto, CA, USA) was used to acquire images. Mice were scanned using a 39mm diameter quadrature birdcage volume coil (Rapid Biomedical GmbH, Wurzburg, Germany). Power calibration and global shimming were performed followed by a series of pilot transverse images acquired over the heart. The apex and mitral valve planes were viewed using single coronal and sagittal images. These images were used to plan the true short axis plane. To measure ventricular function 12-13 contiguous short axis slices were obtained to cover both the right and left ventricles using a spoiled gradient-echo cine sequence (TR=5ms, TE=1.42MS, flip angle 15°, FOV 30x30mm, data matrix 128x128, 1mm slice thickness). Images were ECG triggered to the R wave with a cine delay of 15ms with approximately 30 phases acquired over one cardiac cycle. Images were zero-filled to a matrix of 256 x 256.


1. Jiao K*, et al.* An essential role of Bmp4 in the atrioventricular septation of the mouse heart*. Genes Dev*. 2003;17(19):2362-7.
2. Merki E*, et al.* Epicardial retinoid X receptor alpha is required for myocardial growth and coronary artery formation*. Proc Natl Acad Sci U S A*. 2005;102(51):18455-60.
3. Zhou B*, et al.* Epicardial progenitors contribute to the cardiomyocyte lineage in the developing heart*. Nature*. 2008;454(7200):109-13.
4. Kobayashi K*, et al.* Survival of developing motor neurons mediated by Rho GTPase signaling pathway through Rho-kinase*. J Neurosci*. 2004;24(14):3480-8.
5. Srinivas S*, et al.* Cre reporter strains produced by targeted insertion of EYFP and ECFP into the ROSA26 locus*. BMC Dev Biol*. 2001;1(1):1-4.